Research article

X-RAY SPECTROMETRY

Received: 22 June 2016 Revised: 22 August 2016 Accepted: 23 August 2016 Published online in Wiley Online Library: 27 September 2016

(wileyonlinelibrary.com) DOI 10.1002/xrs.2711

Thickness determination of gold layer on pre-Columbian objects and a gilding frame, combining pXRF and PLS regression

Fabio Lopes,[a]* Fabio Luiz Melquiades,[a] Carlos Roberto Appoloni,[a] Roberto Cesareo,[b] Marcia Rizzutto[c] and Tiago F. Silva[c]

In conservation, restoration and characterization studies of art and archaeological objects, the improvement of analytical techniques is a tendency. X-ray fluorescence (XRF) is a versatile technique, and it has been widely used in the last decades for characterization of a great variety of materials (metals, glass, paints, inks, ceramics, etc.) applied to cultural heritage studies. Besides the chemical composition, it is possible to infer the layer thickness through XRF, enabling a general knowledge of the manufacturing techniques implemented by the culture of origin, as well as the association with the technological level reached for the production of each kind of artefact. The aim of this study is to introduce an alternative way for gold thickness determination of coatings in cultural heritage objects, combining portable XRF data and partial least square regression. As a case of study, we present the use of this methodology in portable XRF measurements performed *in situ* on a gilding frame in Brazil and in two pre-Columbian artefacts from Chavin culture in Peru. Gold layers with thicknesses determined by Rutherford backscattering spectrometry (RBS) were used as standards to perform a calibration model and to check the methodology before its application to unknown artefacts. Copyright © 2016 John Wiley & Sons, Ltd.

Introduction

Many analytical techniques have been widely used in the last decade for the studies and characterizations of archaeological and historical objects of art, especially the X-ray fluorescence (XRF), its variant portable XRF (pXRF), particle-induced X-ray emission and instrumental neutron activation analysis), which are all adequate techniques for these kinds of studies due to the quantity and quality of information that can be obtained on the elemental composition of objects.[1–3]

In this list, XRF is a versatile technique that combines a non-destructive, well-established technique, with high analytical sensitivity that allows simultaneous multi-elemental analysis with low cost and simple instrumentation. Thus, the technique is particularly suitable for archaeological studies where the characterization of materials or process is specially important.[4–6] In recent years, the use of pXRF has increased in museums, churches and excavations due to its portability.[7–9]

In fact, the characterizations of metallic pieces are among the most prominent applications of PXRF in archaeometry and cultural heritage, in particular characterization of pre-Columbian alloys, golden or silvered objects and pigment analysis.[10–17]

However, it is also possible to analyse the layer thicknesses, allowing the study of manufacturing techniques or even the technological level reached to produce each kind of artefact. A method commonly used for thickness determination is differential attenuation, in which the net intensity of Kα and Kβ peaks of the elements of interest in the layer and in the base of the work of art is determined.[18–23] Another possibility is the use of multivariate statistics to obtain the same information.

It is known that the concentration and other sample information are proportional to the peak intensity and sometimes to the scattering peak intensity. The use of multivariate statistics improves data interpretation, enabling the determination of implicit information.

This study aim is to introduce an alternative way for gold thickness determination of coatings in cultural heritage objects, combining pXRF data and partial least square (PLS) regression. As a case study, we present the use of this methodology in pXRF measurements performed *in situ* on different objects, including a gilded frame in Brazil that was in restoration process and knows that the thickness is important for proper restoration, and in two pre-Columbian artefacts from Chavin culture in Peru, where there was a doubt about the method of manufacturing. Gold layers with thicknesses determined by Rutherford backscattering spectrometry (RBS) were used as standards to perform a calibration model and to check the methodology before its application to unknown artefacts.

* *Correspondence to: Fabio Lopes, Laboratório de Física Nuclear Aplicada, Departamento de Física, Universidade Estadual de Londrina, Campus Universitário, Caixa Postal 10011, CEP: 86057-970, Londrina, PR, Brazil. E-mail: fabiolopes@uel.br*

a *Laboratório de Física Nuclear Aplicada, Departamento de Física, Universidade Estadual de Londrina, Campus Universitário, Caixa Postal 10011, CEP: 86057-970, Londrina, PR, Brazil*

b *Instituto di Matematica e Fisica, Università degli Studi di Sassari, Via Vienna 2, 07100, Sassari, Italy*

c *Instituto de Física da Universidade de São Paulo, Rua do matão, travessa R 187, CEP 05508-090, São Paulo, Brazil*

Material and methods

Art artefacts

In this study, we evaluated three different artefacts: (1) the Au over Pb case in the frame of a painting, (2) the Au over Cu case in an artefact formed by six small heads from Chavin culture and (3) the Au over Ag case in a golden vessel also from Chavin culture. The painting of the first case is entitled 'Mulher enxugando o braço esquerdo' ('Woman wiping her left arm'), dating from 1884 and attributed to Hilaire-Germain Edgar de Gas, which belongs to the Museum of Art of São Paulo Assis Chateaubriand (MASP) in Brazil. Both metallic alloy samples belong to the Enrico Poli Museum, in Lima Peru. The pXRF data for these three samples were compared by using the conventional approach by differential attenuation methodology[24,25] and PLS regression.

Instrumentation

For in-field measurements, two different in-house designed systems were used accordingly to their availability in the measurement occasion – one for the paint and another for the metallic alloys.

System 1—frame

The pXRF system used for the measurements performed in Brazil, at MASP, is mounted in a specially designed mechanical system with 45° for incidence and 45° for detection, both referred from the normal to the surface of the sample. It enables angular and translational movements of the excitation-detection system in respect to the measurement spot, making the system optimized for archaeometry measurements. A Magnun MUHV50 mini X-ray tube, with Ag target, controlled by an external high voltage source (configured to work with 35 kV and 5 μA) with a 100-μm Ag filter composes the system. The detector was the XR-100CR, with 6-mm^2 active area, 12.5-μm Be window with 140-eV resolution at 5.9 keV Mn-Kα.[26] The distance between the frame and detector was 2.4 cm and measurement time was 300 s.[27,28]

System 2—metallic alloys

For the measurements performed at Enrico Poli Museum, Lima, Peru, a portable X-ray tube was used: model Mini X with Ag target (configured to work with 35 kV and 5 μA). The detector was a Si-Drift, model X-123SDD with 7-mm^2 active area, 12.5-μm Be window and 125-eV resolution at 5.9 keV for Mn-Kα. The X-ray tube was placed at 55° and the detector at 90°, both angles referred to the normal to the sample surface. The artefacts were placed approximately 1.5 to 2.5 cm away from the measurement system. The variation in the distance is due to the shape and morphology of the studied artefacts. The measurement time was also variable, which ranged from 50 to 200 s.[24,25]

Differential attenuation: (Kα/Kβ) and (Lα/Lβ)

Thin coating layers of metallic elements, e.g. superimposed foils, like gold thin foils, decorative pigments in ceramics and Tumbaga technique, can be determined calculating the differences in the attenuation of emitted K and L characteristic X-ray lines from deeper interfaces. Figure 1 presents the scheme of the measurement concept, considering an artefact made of a base composed by the element 'a' (copper for example), covered by a thin layer of a single element 'b' (gold for example). The ratio of intensities of the K characteristic lines $\left(\frac{K\alpha}{K\beta}\right)$ emitted by element 'a' from the base layer depends on the thickness of element 'b'. The same is valid for the ratio of intensities for the L characteristic lines $\left(\frac{L\alpha}{L\beta}\right)$.[29] These ratios are of fundamental importance in the pictoric layer analysis in paintings, golden and silvered artefacts and other samples, which contain more than two elements.

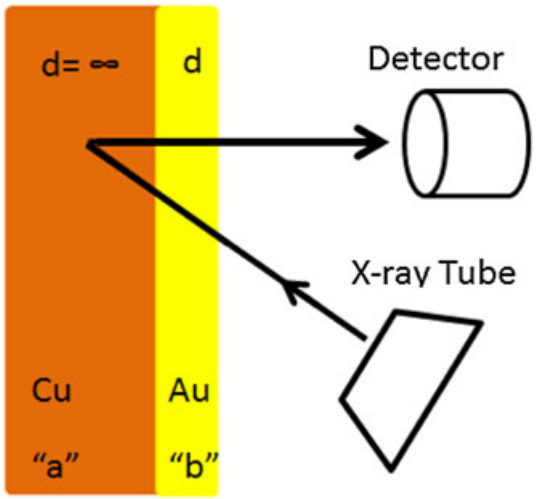

Figure 1. Illustrative scheme representing copper over gold attenuation.

When characteristic X-ray from K or L lines of an element crosses another element layer, the ratio between changes due to different attenuations for the different energies of K_α, K_βe Lα, L_β lines. This attenuation is denoted as differential attenuation and is given by Eqns (1) and (2), called as *R* in this study:

$$R_K = \left(\frac{K\alpha}{K\beta}\right)_\infty e - (\mu 1 - \mu 2)\rho d \quad (1)$$

$$R_L = \left(\frac{L\alpha}{L\beta}\right)_\infty e - (\mu 1 - \mu 2)\rho d \quad (2)$$

where $\left(\frac{K\alpha}{K\beta}\right)_\infty$ and $\left(\frac{L\alpha}{L\beta}\right)_\infty$ are the ratio for the base material of infinite thickness; μ_1 is the linear attenuation coefficient for the coating material at the *Kα* energy (cm^{-1}); μ_2 is the linear attenuation coefficient for the coating material at the *Kα* energy (cm^{-1}); ρ is the material density (g cm^{-3}); *d* is the thickness of the coating layer (cm).

The ratios $\left(\frac{K\alpha}{K\beta}\right)_\infty$ and $\left(\frac{L\alpha}{L\beta}\right)_\infty$ represent the material ratio modified by the self-absorptions that are available in form of tables or need to be determined experimentally.[30] For instance, for Cu and Ag, these ratios $\left(\frac{K\alpha}{K\beta}\right)_\infty$ are 5.1 and 6.9 respectively.[24,25] For Pb, the ratio $\left(\frac{L\alpha}{L\beta}\right)_\infty$ is approximately 1.83.[28] All the spectral analyses to obtain the net area of the peaks were performed with WINQXAS software.

RBS measurements

The RBS is a nuclear technique used to determine and quantify the chemical elements present in a sample with sensitivity of approximately 0.1%. Based on the analysis of energy spectra of energetic ions scattered by the sample atoms, it can provide information on depth profile and thicknesses of layers up to thousands of micrometres, depending on the combination of incident ion, ion

energy and material composition. The RBS measurements in this study were performed by analysing the energy spectra of backscattered protons to 170° scattering angle, with 2.2-MeV incidence energy. Typically, an RBS measurement provides the thickness of layers in areal density units, which in our case were converted to micrometre units by using the gold density of 19.30 g/cm^3, and these data were used in the calibration step of the analysis.

The PLS regression

Among the quantitative multivariate analysis methods, the PLS regression has been widely used for spectra data evaluation and is a well-known factorial analysis applied to parameter modelling, including several applications in archaeometry[31–35] and also in XRF to predict physic-chemical parameters.[36–38]

Partial least square regression establishes a quantitative relationship between the set of instrumental responses (matrix X), for example, the spectra data, with one or more physical or chemical properties of the samples (matrix Y), as for example, the concentration, viscosity, acidity, etc., resulting in a mathematical model that correlates such information. The procedure of using PLS regression comprises two steps: calibration and validation. Calibration step concerns in establishing a relation between the data matrix X (instrumental signals and independent variables) and the known sample properties using reference samples (dependent variables) organized in the matrix Y. The validation step allows for verification if the model is capable of predicting the properties of new samples. The metric applied to measure the model performance is the evaluation of the root mean square error of calibration (RMSEC) and the root mean square error of validation (RMSEP) in each data set.[39] MATLAB software with PLS toolbox pack was used for the data treatment.

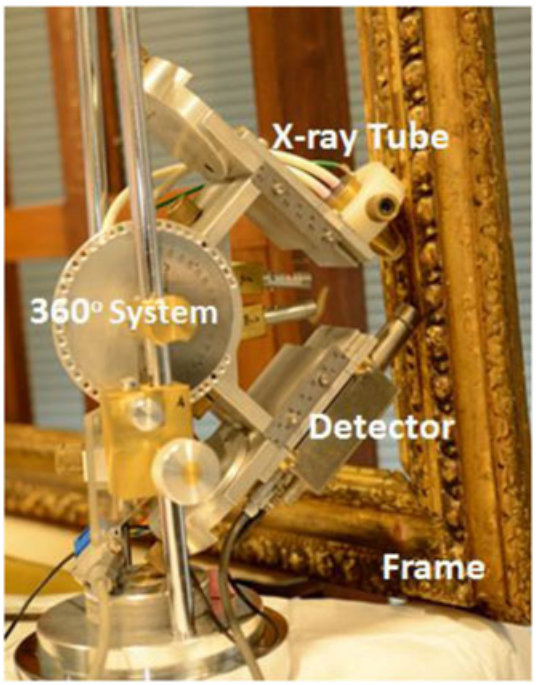

Figure 2. pXRF system measuring the frame at *Museu de Arte de São Paulo*, Brazil.

Multilayered artefacts

Frame of painting (the Au over Pb case)

The 58 × 64-cm frame of the painting by Hilaire-Germain Edgar de Gas was analysed (Fig. 2). It is known that the frame is made of wood with a base of white lead, covered with golden details.[28] Six points were chosen for the pXRF measurements. The criteria used for point selection took into consideration the search of an irradiated surface as plane as possible and with no apparent failure in the golden layer, i.e. with no visible white background. Each point was measured during 300 s.

To obtain a standard for this analysis, Pb metallic plates covered with Au foils were produced. The total thickness of Gold covering was sequentially incremented by using 1, 2, 6, 12 and 22 foils. Each foil has 0.094 μm, measured by RBS, corresponding to 0.094, 0.188, 0.564, 1.128 and 2.068 μm respectively. The same standards were measured by using the pXRF; each standard foil was measured five times, during 500 s each, and the average spectra used in the calibration. The measurement conditions were the same used at MASP, using system 1.

For the PLS regression, the calibration spectra data were arranged in a 5 × 1024 matrix (X) and a 5 × 1 matrix (Y) with the thickness values. The validation data were arranged in a 6 × 1024 matrix (X) with the spectra from the frame of the paint. The mean centre was used as a pre-processing step, and all spectra were normalized to the same measurement time.

Six small heads (the Au over Cu case)

Figure 3 presents a pre-Colombian artefact formed by six small heads, from Enrico Poli Museum of Lima, Peru, which is a piece in

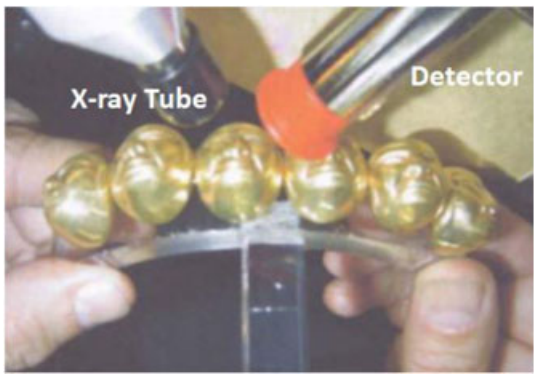

Figure 3. Six small golden heads. Chavin culture. Image from Enrico Poli Museum, Peru.

Figure 4. Tumbaga vessel in silver. Chavin culture. Image from Enrico Poli Museum, Peru.

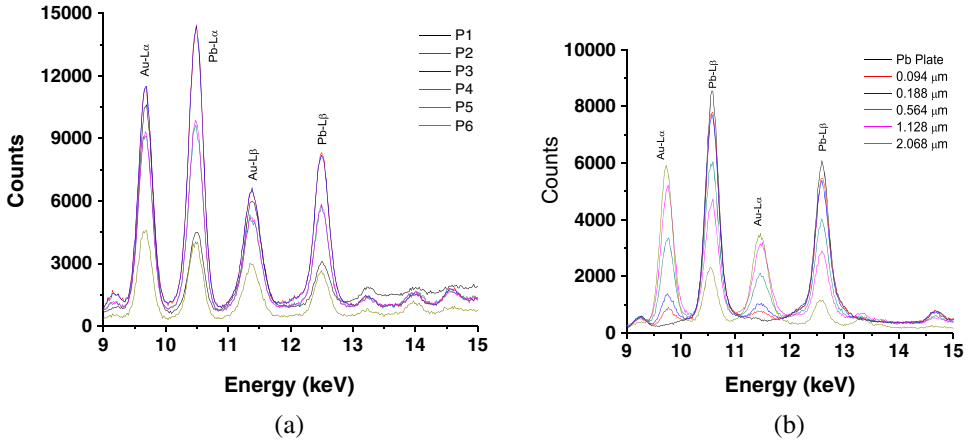

Figure 5. Spectra data from (a) the sample for thickness prediction (frame) and (b) Au foils over Pb metallic plate as standards for calibration.

excellent condition of preservation. Previous studies using pXRF analysis showed that it is an alloy rich in Cu. In fact, it has just a small covering of Au, produced with Tumbaga technique.[24,25] Each head of the artefact was measured by pXRF during approximately 200 s. The data set was normalized to the same measuring time before the PLS regression analysis.

The Au–Cu standards for calibration were made by using the same methodology, as for the frame case, by covering copper plates with Au foils. The thickness of the gold cover was also sequentially incremented by using 1, 2, 4, 6, 8, 16 and 32 foils. This time, each foil has 0.125 μm thickness, measured by RBS. The standards have 0.125, 0.250, 0.500, 0.750, 1.000, 2.000 and 4.000 μm thicknesses respectively. The same standards were measured by using the pXRF; each sample was measured thrice, in different days, during 100 s. The experimental setup was the same as described in the section on Art Artefacts.

For the PLS regression analysis, the spectra of the standards were arranged in a 7×1024 matrix (X) and the thicknesses in a 7×1 matrix (Y) corresponding to the calibrated values. The validation data were arranged in a 6×1024 matrix (X), referring to the spectra of each head and the Y matrix that shall be the predicted by the PLS regression model. In all data, the mean centre was applied as a pre-processing step.

Golden vessel (the Au over Ag case)

The vessel presented in Fig. 4 has a golden aspect and belongs also to the Enrico Poli Museum of Lima, Peru. The archaeological data indicate that it was produced by the Chavin culture. This sample was previously evaluated, showing the presence of Ag–Au–Cu alloy attributed to the Tumbaga method of manufacturing.[24,25]

The standards for calibration in this case were also made by superposition of Au foils on an Ag metallic plate. The thickness was sequentially incremented by using 1, 3, 5, 7, 11, 13 and 15 foils. Each foil has 0.125 μm thicknesses, measured by RBS, corresponding to 0.125, 0.375, 0.625, 0.875, 1.375, 1.625 and 1.875 μm standard thicknesses respectively. The same standards were measured by using the pXRF; each sample was measured thrice, in different days, during 100 s. The experimental setup was the same describe on the section on Art Artefacts for system 2. Three regions of the vessel were measured, and the spectra data were used in the PLS regression.

The calibration data were arranged in a 7×1024 matrix (X) with the spectra data and a 7×1 matrix (Y) with the thickness values. The validation matrix with the spectral data was arranged in a 3×1024 matrix (X) relative to the three measurements of the vessel.

Results

Frame of XIX century paint (the Au over Pb case)

Despite all the efforts to avoid geometry problems, there is no complete flat surface in the frame (Fig. 2). Because the X-ray spot was a

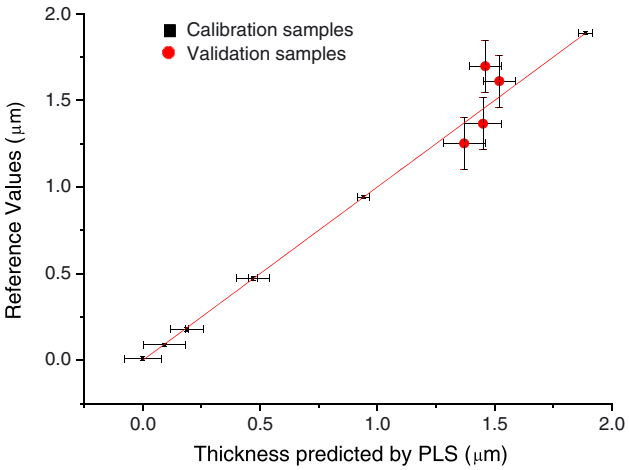

Figure 6. PLS regression curves for calibration and validation samples for the frame of paint. Values in μm. The error bars indicate the estimated error with 95% confidence level.

Table 1. Thickness for the frame points determined by the two methodologies

Sample	Measured by differential attenuation (μm)	Predicted by PLS (μm)
P2	1.45 ± 0.08	1.36 ± 0.15
P3	1.37 ± 0.09	1.25 ± 0.15
P4	1.46 ± 0.07	1.70 ± 0.15
P5	1.52 ± 0.07	1.61 ± 0.15
Average	1.45	1.48
Standard deviation	0.06	0.21

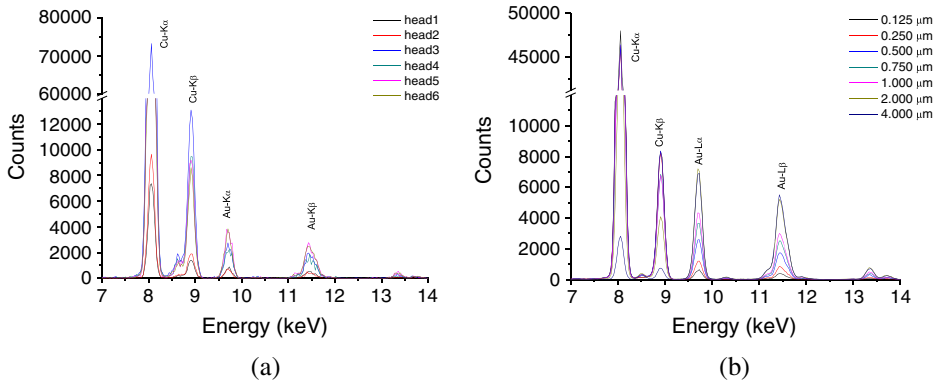

Figure 7. Measured spectra from (a) each small golden head and (b) Au foils over Cu metallic plate used for calibration.

circle of approximately 5 mm diameter, some differences in the observed background could not be completely avoided. Figure 5(a) presents the spectra of all measured points.

Based on differences visually perceived and confirmed by PCA analysis (not shown), points P1 and P6 were excluded because the data were very different from the others, probably due to the geometry problems mentioned in the preceding texts. Another reason for that could be an eventual variation of the thickness in the Pb preparation layer under the gold covering, generating spectrum variations. It can be noticed in Fig. 5(a) how the Pb peak intensities are low for the P1 and P6 measurements when compared with the other points. Figure 5(b) demonstrates the spectra of Au foils over Pb metallic plate standards.

Several different models of PLS regression were tested to check for consistency – some considering the full range of the spectra and others considering just the range with the Au and Pb peaks – as detailed in Fig. 5(b). In this consistency check, the hole of some pre-processing steps was also evaluated. Finally, the best model considered the region of the spectra that begins at 9 keV and goes up to 14 keV, using mean centre as a pre-processing step. This model, with three latent variables, was able to explain 99.85% of the data variance.

Figure 6 presents the regression curve with the calibration and prediction points. The values for RMSEC and RMSEP are 0.01 and 0.15 respectively. The same data were assessed by the conventional approach of differential attenuation.[28] These values are compared with the values determined by PLS regression in Table 1. The relative difference of both methods stays between 6 up to 16%, and the thickness values could be considered equivalent, within the error bars.

The six small heads (the Au over Cu case)

This artefact is considered a complex example to be measured by pXRF. Its reduced size and the refinement in detail make the reproducibility very difficult. There is no flat region to perform the measurements; thus, the distance between sample and PXRF system could not be kept the same for all measures. Figure 7(a) presents the spectra obtained for the six points. The best PLS regression models for this artefact were obtained by assuming the region from 9.3 to 14 keV that contains the Au peaks [Fig. 7(b)]. *Lα and Lβ peaks are the most relevant for PLS regression, while the Lγ line has minor importance*. Additionally, the calibration was performed by using up to 32 overlapped Au foils.

The PLS regression model with three latent variables was explained over 99% of the variance. The determination coefficient for the calibration data was 0.998 and for the prediction data was 0.54, which means that standard and sample spectra are quite different (Fig. 8). We attribute this issue to geometry reproducibility, as mentioned in the preceding texts. The RMSEC and RMSEP values were 0.04 and 0.42 respectively. Nevertheless, the relative deviation, compared with the results determined by using the conventional approach by differential attenuation methodology,[24,25] was approximately 25%, except for head 4 case (Table 2) that showed the results in the same order of magnitude. Spectra from

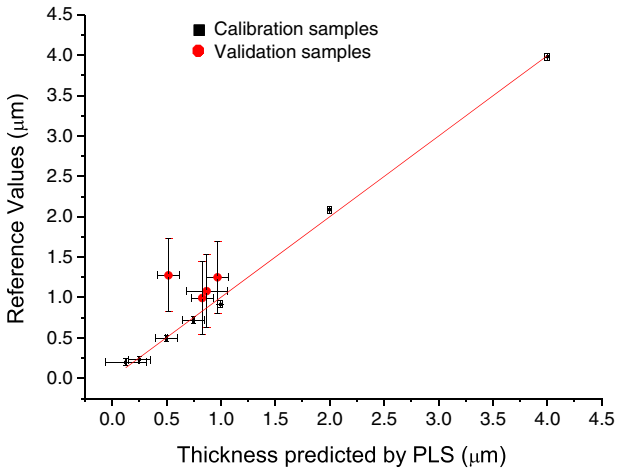

Figure 8. PLS regression curves for calibration and validation samples for the six heads. Values in μm. The error bars indicate the estimated error with 95% confidence level.

Table 2. Thickness for the golden six heads determined by the two methodologies

Samples	Measured by differential attenuation (μm)	Predicted by PLS (μm)
Head 3	0.87 ± 0.19	1.08 ± 0.42
Head 4	0.52 ± 0.10	1.27 ± 0.42
Head 5	0.83 ± 0.10	0.99 ± 0.42
Head 6	0.97 ± 0.10	1.25 ± 0.42
Average	0.80	1.15
Standard deviation	0.19	0.14

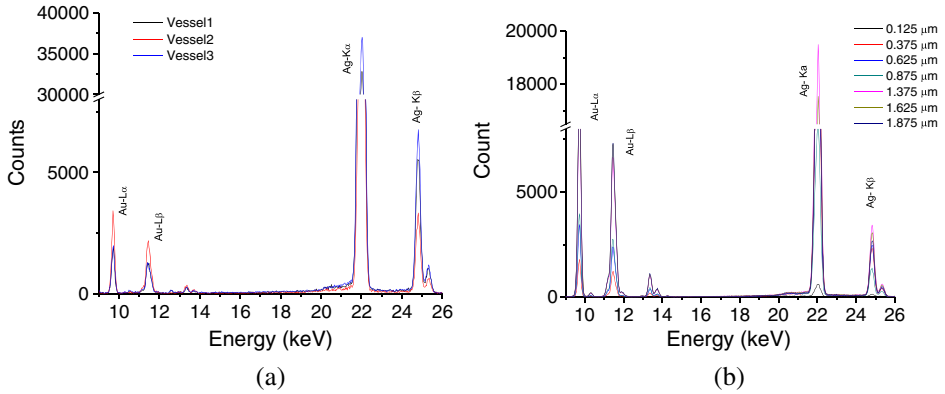

Figure 9. Measured spectra from (a) each point in the vessel and (b) Au foils over Ag metallic plate used for calibration.

samples 1 and 2 were excluded from the analysis due to very low intensities of Cu and Au peaks when compared with the other spectra, and the reasons for that is again the geometry reproducibility.

Golden vessel (the Au over Ag case)

This artefact can be considered a homogeneous base of metallic Ag covered by a thick Au layer, probably manufactured by Tumbaga techniques. However, its surface presents some roughness and non-uniformities, which increases X-ray scattering. Figure 9(a) presents the spectra from the three measured points – two in the outer side and one on the inner side of the vessel. The best PLS regression model was obtained by assuming the region of the spectra from 18 keV up to 30 keV, which contains the Ag peaks [Fig. 9(b)].

The calibration was performed by using the data for samples with up to 15 overlapped Au foils. The model with three latent variables explained 99.7% of the variance. The determination coefficient for the calibration curve was 0.970 and for the prediction data was 0.983 (Fig. 10). Although the prediction curve is well explained by the model, the relative deviation compared with the conventional approach using differential attenuation varied from 10 to 40% (Table 3). The RMSEC and RMSEP values were 0.08 and 0.32 respectively.

It is worth mentioning that, in the vessel, the Au layer over the Ag base is apparently not so homogeneous and it presents some flaws

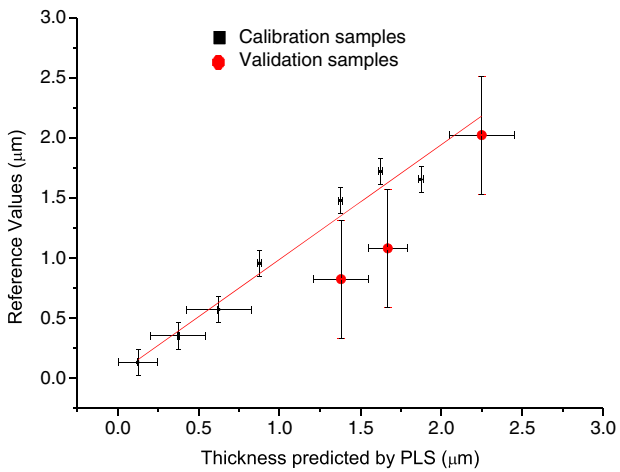

Figure 10. PLS regression curves for calibration and validation samples for the vessel. Values in μm. The error bars indicate the estimated error with 95% confidence level.

Table 3. Thickness for the vessel determined by the two methodologies

Samples	Measured by differential attenuation (μm)	Predicted by PLS (μm)
Vessel 1	1.67 ± 0.12	1.08 ± 0.49
Vessel 2	1.38 ± 0.17	0.82 ± 0.49
Vessel 3	2.25 ± 0.20	2.02 ± 0.49
Average	1.77	1.31
Standard deviation	0.44	0.63

in the surface that makes some silvered dots visible. The X-ray spot used in these analyses had an area wide enough to cover a region that contains some of these flaws; this contributes to the large uncertainties in the thickness prediction.

Discussion and conclusions

These deviation ranges are in the same order of magnitude compared with typical values of uncertainties. The relative deviation of the results obtained by the PLS regression approach when compared with the conventional approach using the differential attenuation methodology ranged from 6 to 16% for the frame of the painting, from 20 to 29% for the six small heads and from 10 to 40% for the vessel obtained by using the differential attenuation methodology,[24,25] which leads us to conclude that both methodologies can be used. Indeed, the R^2 for the thickness prediction curves obtained by PLS regression ranged from 0.86 to 0.98 and can be improved by setup optimizations, choice of flat spots and higher counting statistics, reflected by higher measurement times.

The robustness of the models could be evaluated by the RMSEC and RMSEP values. The optimum number of latent variables in each model was chosen based on a plot of these values (RMSEC and/or RMSEP vs number of latent variable, not presented).[40] All the models presented the best results for three latent variables. It is possible to assure that exceeding this number, the gain is inexpressive because the standard deviation is stabilized. Also, it is possible to verify that the RMSEC value is an order of magnitude smaller than the RMSEP, indicating that the calibration correlation is very satisfactory while the external validation has higher standard deviation values as could be attested in Figs 6, 8 and 10.

The direct use of the spectra is one of the advantages of the PLS regression methodology for the determination of gold thickness of

the covering layers because it is not necessary to process the spectra in order to obtain the peak net area and Kα/Kβ ratios. Eventually, some pre-processing step may be necessary in the PLS regression, but depending on the software used for the data processing, this task can be no time consuming at all. Additionally, the use of standards to produce a calibration curve for the PLS regression model makes this approach insensitive to eventual errors in the attenuation database, and for well-stable devices, this calibration can be carried out just once.

One disadvantage presented during this study is the sensitivity to experimental reproducibility, which can be circumvented by improvements in the alignment procedure. In general, it is possible to conclude that PLS regression combined with pXRF is a viable alternative for thickness determination in golden surfaces for a wide variety of materials and geometries.

Acknowledgements

Fabio Lopes acknowledges CAPES Brazilian funding agency for eight months of PhD grant during his stay at the Instituto di Matematica e Fisica, Università degli Studi di Sassari, Sassari, Italy.

References

[1] D. Agha-Aligo, P. Oliaiy, M. Mohsenian, M. Lamehi-Rachti, F. Sholoyhi. Provenance study of ancient Iranian luster pottery using PIXE multivariate statistic analysis. *J of CultHeritage* **2009**, *4*(10), 487–492.
[2] T. Calligaro, J. C. Dran, M. Klein. Application of photo-detection to art and archaeology at the C2RMF. *Nucl Instrum and Meth In Phys A* **2003**, *504*, 213–221.
[3] M. Ferretti. Fluorescence from the collimator in Si-PIN and Si-drift detectors: problems and solutions for the XRF analysis of archaeological and historical materials. *Nucl Instrum and Meth In Phys B* **2004**, *226*(3), 453–460.
[4] M. L. Carvalho, M. Manso, S. Pessanha, A. Guilherme, F. Ferreira. Quantification of mercury in XVIII century books by energy dispersive X-ray fluorescence (EDXRF). *J of Cult Herit* **2009**, (10), 435–438.
[5] T. Cechák, M. Hlozek, L. Musílek, T. Trojek. X-ray fluorescence as a tool for investigating archaeological finds. *Nucl Instrum and Meth In Phys A* **2007**, (580), 717–720.
[6] S. Shalev, S. S. H. Shilstein, Y. U. Yekutieli. XRF study of archaeological and metallurgical material from an ancient copper-smelting site near Ein-Yahav. *Israel Talanta* **2006**, (70), 909–913.
[7] M. Aceto, A. Agostinho, E. Boccaleri, A. C. Garlanda. The Vercelli Gospels laid open: an investigation into the inks used to write oldest gospels in Latin. *X-ray Spectrometry* **2008**, (37), 286–292.
[8] C. R. Appoloni, F. Lopes, F. L. Melquiades, C. I. Parellada. *In situ* pigments study of rock art at Jaguariaíva 1 archaeological site (Parana, Brazil) by portable energy dispersive X-ray fluorescence (EDXRF). *FUMDHAMENTOS* **2010**, (9), 555–562.
[9] A. Gianoncelli, J. Castaing, L. Ortega, E. Dooryhee, J. Salomon, P. Waler, J. L. Hodeau, P. Bordet. A portable instrument for in situ determination of the chemical and phase compositions of cultural heritage objects. *X-ray Spectrometry* **2008**, *37*, 418–423.
[10] R. Cesareo, A. Brunetti. Metal sheets thickness determined by energy dispersive X-ray fluorescence analysis. *J of X-Ray Scien and Techn* **2008**, *2*(16), 119–130.
[11] V. Desnica, K. Skaric, D. Jembrih-Simbuerger, S. Fazinic, M. Jaksic, D. Mudronja, M. Pavlicic, I. Peranic, M. Schreiner. Portable XRF as a valuable device for preliminary *in situ* pigment investigation of wooden inventory in the Trski Vrh Church in Croatia. *Applied Physics A* **2008**, *1*(92), 19–23.
[12] F. P. Hocquet, H. P. Garnir, A. Marcharl, M. Clar, C. Oger, D. Strivay. A remote controlled XRF system for field analysis of cultural heritage objects. *X-ray Spectrometry* **2008**, *4*(37), 304–308.
[13] A. Longoni, C. Fiorini, P. Leutenegger, S. Sciuti, G. Fronterotta, L. Struder, P. Lechner. Portable XRF spectrometer for non-destructive analyses in archaeometry. *Nucl Instrum and Meth In Phys A* **1998**, *409*, 407–409.
[14] K. Uhliir, M. Griesser, G. Buzanich, P. Wobrauschek, C. Streli, D. Wegrzynek, A. Markowicz, E. Chinea-Cano. Application of a new portable (micro) XRF instrument having low-Z elements: determination capability in the field of works of art. *X-ray Spectrometry* **2008**, *37*, 450–457.
[15] M. S. Blonski, C. R. Appoloni. Pigments analysis and gold layer thickness evaluation of polychromy on wood objects by PXRF. *Appl Radiat and Isotopes* **2014**, (89), 47–52.
[16] R. Cesareo, A. D. Bustamante, S. Julio Fabian, C. Calza, M. Anjos, R. T. Lopes, W. Alva, L. Chero, V. F. Gutierrez, M. D. Espinoza, R. R. Rodriguez, M. F. Seclen, V. Curay, C. Elera, I. Shimada. Pre-Columbian alloys from the royal tombs of Sipán and from Museum of Sicán: non-destructive XRF analysis with a portable equipment. *Archéo Sciences* **2009a**, *33*, 281–287.
[17] R. Cesareo, A. Bustamante, J. Fabian, C. Calza, M. Anjos, R. T. Lopes, I. S. Elera, V. Cuary, M. Rizzutto. Energy-dispersive X-ray fluorescence analysis of a pre-Columbian funerary gold mask from the Museum of Sicán. *Peru X-ray Spectrometry* **2010**, (39), 122–123.
[18] J. Salomon, J. C. Dran, T. Guillou, B. Moignard, L. Pichon, P. Walter, F. Mathis. Ion-beam analysis for cultural heritage on the AGLAE facility: impact of PIXE/RBS combination. *Appl Phys A* **2008**, *1*(92), 43–50.
[19] M. I. M. S. Bueno, M. T. P. O. Castro, A. M. Souza, E. B. S. Oliveira, A. P. Teixeira. X-ray scattering processes and chemometrics for differentiating complex samples using conventional EDXRF equipment. *Chemometr Intell Lab Syst* **2005**, (78), 96–102.
[20] C. Vázquez, S. Bocykens, H. Bonadco. Total reflection X-ray fluorescence polymer spectra: classification by taxonomy statistic tools. *Talanta* **2002**, *6*(57), 1113–1117.
[21] R. Cesareo. Thickness and composition of gold and silver alloys determined by combining EDXRF-analysis and transmission measurements. *X-ray Spectrometry* **2014**, (43), 312–315.
[22] A. G. Karydas, R. Padilla-Alvarez, M. Drozdenko, M. Korn, M. O. Moreno Guzmán. Handheld XRF analysis of the old Mexican feather headdress in the Weltmuseum Viena. *X-ray Spectrometry* **2014**, *43*, 138–145.
[23] S. Sofia Pessanha, S. Longelin, A. Le gac, M. Manso, M. L. Carvalho. Determination of gold leaf thickness in a Renaissance illumination using a nondestructive approach. *X-ray Spectrometry* **2014**, *43*, 79–82.
[24] R. Cesareo, A. D. Bustamante, S. Julio Fabian, A. Z. Sandra, W. Alva, L. Chero, M. C. Espinoza, C. R. Rodriguez, M. R. Seclen, F. V. Gutierrez, E. B. Lévano, G. A. Juan, M. Rizzutto, E. Poli, C. Calza, M. Anjos, R. T. Lopes, G. E. Gigante, M. G. Ingo, R. Riccucci, C. Elera, I. Shimada, V. Curay, M. Castillo, F. Lopes. Evolution of pre-Columbian metallurgy from the north of Peru studied with portable non-invasive equipment using energy-dispersive X-ray fluorescence. *J Mater Sci Eng B 1* **2011**, 48–81.
[25] R. Cesareo, A. D. Bustamante, S. Julio Fabian, S. Z. Del Pilar, W. Alva, L. Chero, M. C. Espinoza, R. Rodriguez, M. F. Seclen, V. F. Gutierrez, B. L. J. A. G. Edgard, M. A. Rizzutto, E. Poli, C. Calza, M. Anjos, R. P. Freitas, R. T. Lopes, C. Elera, I. Shimada, V. Curay, F. G. Castilho, G. E. Gigante, G. M. Ingo, F. Lopes, U. Holmquist, D. Diestra. Multilayered artifacts in the pre-Columbian metallurgy from the North of Peru. *Appl Phys A* **2013**, *113*, 889–893.
[26] Ampetek Inc. Home. Disponível em: http://www.amptek.com/.
[27] R. E. Van Grieken, A. A. Markowicz, *Handbook of X-ray Spectrometry*, 2. edn, Marcel Dekker, New York, **2002**.
[28] F. Lopes. Measures of elemental composition and thickness of multilayer metal and pigments of objects in the cultural heritage using portable X-ray fluorescence (PXRF). 2014. 161 p. PhD Thesis Physics — State University of Londrina and State University of Maringá, Londrina, **2014**.
[29] C. R. Appoloni, F. Lopes, M. A. Bruno, in *Análise da pintura "Moema" por PXRF, TXRF e Espectrometria Raman in Moema: restauração* (Ed: K. Barbosa), Comunique Editorial, Brazil, **2013**, pp. 59–79.
[30] T. Trojek, T. Cechak, L. Musílek. Recognition of pigment layers in illuminated manuscripts by means of K_α/K_β and L_α L_β ratios of characteristic X-rays. *Appl Radiat Isot* **2010**, *4*(68), 871–874.
[31] E. Marengo, E. Robotti, M. C. Liparota, M. C. Gennaro. Monitoring of pigmented and wooden surfaces in accelerated ageing processes by FT-Raman spectroscopy and multivariate control charts. *Talanta* **2004**, *4*(63), 987–1002.
[32] A. Pallipurath, R. V. Vőfély, J. Skelton, P. Ricciardi, S. Bucklowd, S. Elliott. Estimating the concentrations of pigments and binders in lead-based

paints using FT-Raman spectroscopy and principal component analysis. *J Raman Spectrosc* **2014**, *45*(201), 1272–1278.
[33] C. Sessa, H. Bagán, J. F. García. Influence of composition and roughness on the pigment mapping of paintings using mid-infrared fiberoptics reflectance spectroscopy (mid-IR FORS) and multivariate calibration. *Anal Bioanal Chem* **2014**, *26*(406), 6735–6747.
[34] E. Marengo, M. C. Liparota, E. Robotti, M. Bobba. Multivariate calibration applied to the field of cultural heritage: analysis of the pigments on the surface of a painting. *Anal Chim Acta* **2005**, *1–2*(553), 111–122.
[35] I. Calliari, E. Canal, S. Cavazzoni, L. Lazzarini. Roman bricks from the Lagoon of Venice: a chemical characterization with methods of multivariate analysis. *J Cult Herit* **2001**, *1*(2), 23–29.
[36] M. I. M. S. Bueno, M. T. P. O. Castro, A. M. Souza, E. B. S. Oliveira, A. P. Teixeira. X-ray scattering processes and chemometrics for differentiating complex samples using conventional EDXRF equipment. *Chemometr Intell Lab Syst* **2005**, *78*, 96–102.
[37] C. R. Appoloni, F. L. Melquiades. Portable XRF and principal component analysis for bill characterization in forensic science. *Appl Radiat Isot* **2014**, *85*, 92–95.
[38] F. L. Melquiades, E. L. Thomaz. X-ray fluorescence to estimate the maximum temperature reached at soil surface during experimental slash-and-burn fires. *J Environ Qual* **2016**, *45*, 1104–1109.
[39] D. L. Massart, B. G. M. Vandeginste, L. M. C. Buydens, S. D. Jong, P. J. Lewi, J. Smeyers-Verbeke, *Handbook of Chemometrics and Qualimetrics*, Elsevier, Amsterdam, **1997**.
[40] R. Bro, Å. Rinnana, N. (. K.). M. Faberb. Standard error of prediction for multilinear PLS 2. Practical implementation in fluorescence spectroscopy. *Chemometr Intell Lab Syst* **2005**, *1*(75), 69–76.